Assiut University Journal of Multidisciplinary Scientific Research (AUNJMSR)
Faculty of Science, Assiut University, Assiut, Egypt.
Printed ISSN 2812-5029
Online ISSN 2812-5037
Vol. 53(2): 217- 237 (2024)
https://aunj.journals.ekb.eg

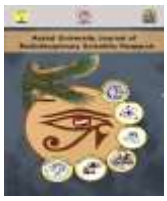

Magnetic survey comparison using smart phone magnetic sensor and proton precession magnetometer: A case study at Abu Marwat Concession, Eastern Desert, Egypt

Mostafa M. Eraky 1*, Gamal Z. Abdelaal 2, Assem E. El-Hadad 3 and Mahmoud H. Elshamy1 4
Geology Department, Faculty of Science, Assiut University, Assiut, Egypt

Email of the corresponding author[1,*]; maeraky@atonresources.com

ARTICLE INFO

Article History:
Received: 2023-12-03
Accepted: 2024-01-15
Online: 2024-04-29

Keywords:

Magnetic,Smart, phonen, application, structure, Nubian Shield

ABSTRACT

Magnetic technique is one of the most effective geophysical methods, with several uses and providing extremely trustworthy information about the subsurface. The main objective of our study is to examine the capability and efficiency of the smart phone application (Physics toolbox magnetometer) to map the depths of the shallow and deep subsurface magnetic features compared with the proton precession magnetometer at Abu Marwat Concession located at Eastern Desert, Egypt. Magnetic data was gathered along 26 profiles with a line spacing of 10m and a station interval of 4m, and the data was processed using the Geosoft Oasis Montaj software (version 8.4). The total magnetic intensity (TMI) map was created, and it was corrected using the reduction to the magnetic pole (RTP) map. The radial average power spectrum technique (RAPS) and source power imaging technique (SPI) were used to measure the depths of shallow and deep magnetic structures. The RAPS technique of the magnetometer revealed that the average depths of shallow and deep magnetic sources are about -4 m and -9 m, respectively. Whereas the smartphone magnetic sensor RAPS results showed -5m and -13m respectively for the depths of shallow and deep magnetic sources. On the other hand, the source power imaging technique exhibited a range from -1.9m and -4.5m for magnetometer versus a depth range from 0.083m to -9.8m for smartphone magnetic sensor. To conclude, the use of smartphone magnetic sensor for shallow depths estimation gives results comparable to that of the magnetometer. Meanwhile, the estimation of the depths of deep structures varies markedly between the two study tools.

1- INTRODUCTION

The magnetic method is a well-known, effective geophysical technique that can provide incredibly useful information below the surface and has a wide range of applications [1]. The use of magnetic method is well known in hydrogeological, geological, and petroleum exploration [2, 3]. Magnetic susceptibility, which varies depending on whether the rock is sedimentary, metamorphic, or pyrotechnic, is used in this procedure. Magnetic characteristics of sedimentary rocks are known to be lesser than pyrotechnic and metamorphic properties in general [4]. The magnetic approach has a number of advantages, including speed and the ability to map magnetic structures close to the surface. However, the approach can only be used to map ferrous materials, and picture resolution degrades rapidly as target depth increases.

To determine the strength and orientation of the Earth's magnetic field, a magnetometer is necessary. Magnetometer surveys, which measure minute, localized variations in the Earth's magnetic field, have an accuracy of 0.002%. Conventional commercial devices are based on the utilization of proton-rich fluids enclosed by an electric coil. Some of these tools are gradiometers, fluxgates, proton precession, and cesium vapor magnetometers. The price of magnetometers on the market nowadays varies depending on the precision and resolution of the magnetic data recorded, and purchasing these devices might be difficult at times. We have lately been able to discover the essential programs on smartphones to perform that operation instead of scientific devices, such as the global positioning system (GPS) application available on smart phones. It is unclear if these applications will be able to do the necessary measurements with sufficient precision and resolution to be comparable to or close to scientific magnetometers. With the advancement of technology, smart phones have

been well-equipped with a variety of novel accessories such as GPS antennas, gravity, light detection, and magnetic sensors [5]. Although manufacturers are competing fiercely to upgrade smartphone sensors, it is unclear how successful these sensors will be in geophysical research. [6]. This is most likely owing to the complexity of geophysical objects, where information about physical properties is encoded in data in a convoluted manner. The present study was carried out at Rodruin prospect area of Abu Marwat Concession, Eastern Desert, Egypt. It comprises an area of 7500 m² and limited by the latitudes 2913040 ,2913150 Northing and the longitude 552400,552650 Easting (Fig.1). The main objective is to inspect the effectiveness of a smartphone sensor, particularly a magnetic sensor in comparison to a magnetometer for geophysical exploration of the depths of shallow and deep magnetic features. Therefore, we made the decision to carry out the experiment. We find it simple to download one of the free applications, use it at a research location with some surface and subsurface magnetic structures, and compare the results with those from a magnetometer.

Figure 1: Location map of the study area at Abu Marwat Concession Rodruin prospect.

2- Previous Studies

Eraky et al. [7] demonstrated the use of the smartphone magnetic sensor (Physics toolbox magnetometer) on a research area at Assiut University's Faculty of Science. The primary goal was to examine the efficiency and capabilities of the smart phone application in mapping the depth and location of near surface magnetic features (e.g., utilities) at the study site. The results obtained with the smart phone application were capable of mapping the .underlying geometries and depths of the pipelines to a greater extent

Ndiaye et al. [8] used an iPhone 4S integrated magnetic sensor to conduct a geomagnetic examination. The examined area has fractured sedimentary terrain with basaltic volcanic veins running across it. The magnetic anomaly map produced illustrates the boundaries between sedimentary rocks and a magnetic body at a certain depth. These results are compared to the magnetic body's shape as depicted by geological maps. The results appear to be correct .in terms of determining the geometry and depth of the magnetic body

N. Campbell et al. [9] investigated the effectiveness of a magnetic field sensor embedded in a smartphone to fill this knowledge gap. A preliminary experiment was carried out using a free application called Andro Sensor to map subterranean pipes at a test site and to assess the performance of the AK09911C magnetic field sensor inside a Samsung Galaxy Note 4 (Android OS) smartphone. In addition, for comparison, data was collected over the test location using the commercially available Geometrics G858 Cesium vapor magnetometer. The smartphone Resu Geometrics was able to locate all three buried pipelines and outperformed the Geometrics G858. A walking survey over a landfill was done for the major experiment to compare the smartphone

to the G858 Cesium vapor magnetometer. Results showed little variation between the G858 Cesium vapor magnetometer and smartphone magnetic .field sensors when within the boundaries of the landfill

Vo et al. [10] used remote magnetic field measurements from above ground magnetometer surveys to detect the depth and position of buried pipes. The calculation is presented and validated by experimental results on steel vessels measuring 152 mm (6 in.). Field experiments against industrial pipe locators are also used to assess the technique's performance. So far, the proposed technique's depth measurement has indicated a potential inaccuracy of 8%. The suggested technique, which generates a three-dimensional profile of underground pipes using rapid above-ground surveys, can be used as a screening technique for asset and integrity management, such as monitoring .geohazard situations

Joshua et al. [11] performed a ground magnetic survey in Tajimi, Lokoja, Kogi State, Nigeria. The study's goal is to pinpoint the location of iron-deposited minerals inside the study area. In the 140m by 75m study area, fifteen magnetic transverse lines were created in an E-W orientation. Data was collected and recorded using a Proton Precession magnetometer; the data was displayed in magnetic profiles, 2D contour maps, and 3D surface maps to aid in qualitative interpretation. The estimated depths of the magnetic source body/rocks from the Earth's surface range from 1.28m to 13.57m, indicating that the magnetic source body assumed to be magnetic mineral is close to the Earth's surface.

3- GEOLOGICAL SETTINGS

Rodruin is located about halfway between the Red Sea and the Nile Valley, roughly in the Centre of the exposed Neoproterozoic Arab-Nubian Shield (ANS) on the Egyptian side of the Red Sea. The ANS consists of a series of accretionary island arc terrains of Neoproterozoic age. As such it would be expected to consist of a large portion of intermediate volcanic rock, deep water trench sediments and abducted ophiolitic material in the fore arc facies and more felsic volcanics, finer volcanoclastic and terrestrial sediments in the back arc basins. The area to the south of Rodruin appears to consist of mostly basic to intermediate volcanics with coarse monomict tuff breccias suggesting they were proximal to active volcanism [١٢].

The geological setting of Rodruin (Fig. 2), apart from it being part of the greater Arab-Nubian accretionary terrain, is rather obscure. The surrounding area for at least 2-3 km in all directions comprises low grade regionally meta morphed “slates” of predominately volcano-sedimentary affinities. From the recent satellite image there appear to be two parallel, linear, features trending roughly WNW-ESE through the immediate Rodruin area. They are about 850m apart at this point and all known mineralization is confined to the zone between them.

To the south of Rodruin the rocks consist mainly of andesitic to basaltic tuffs and tuffaceous sandstones, minor intrusive bodies ranging from pale felsic to dark mafic dykes and stocks. Flows, if present, have not been identified in the field. The presence, however, of large areas of course monocytic tuff breccias suggest they these rocks were proximal to active volcanism. The are no plutonic rocks associated with the "slate" sequence south of Rodruin. Many of the coarser intrusive have diffuse, brecciated margins characterized by epidote rich

breccias. These are interpreted as shallow, hypabyssal intrusive into wet, unlithified or weakly lithified sediments. These rocks appear to form the .footwall to the mineralization

To the north of the mineralized zone there is a thick and monotonous package of more felsic volcanic consisting of scattered dome-like bodies of porphyritic rhyolite and dacite hosted by their equivalent lapilli tuffs, tuffaceous sandstone, .and enigmatic carbonate bodies

The mineralization is hosted by what is probably a fairly thin unit of coarse water lain andesitic tuff, tuffaceous sandstone, siltstone, mudstone and carbonates. However, even the clastic sediments are often rich in carbonate (dolomite) too. No other feature of the geology at Rodruin has solicited so much discussion as the origin and nature of the carbonate facies and the carbonate rich clastic sediments. This enigma will be discussed at length in the following text. If the origin of the carbonate is the most hotly discussed topic amongst Aton's geologist, the controls on and the nature of the mineralization is a close second.

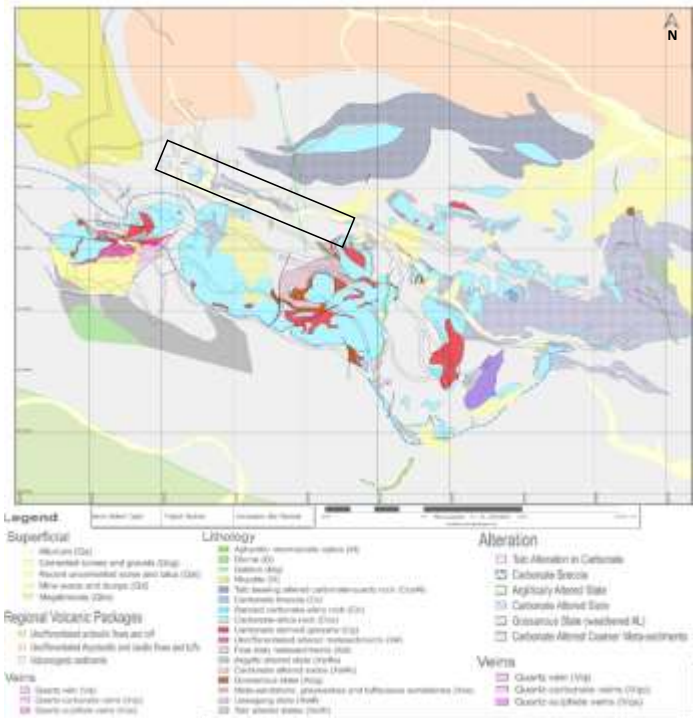

Figure 2: Geologic map for Rodruin prospect with the structure zones.

4- MATERIALS AND METHODS

Geomagnetic investigation was accomplished using smartphone magnetic sensor and magnetometer. The magnetometer device that has been used is (G-858) and smartphone application called The Physics Toolbox gathers data from all mobile sensors, including magnetic, proximity, GPS, and other types. On an iPhone 7 plus, we utilized the free edition of Physics Toolbox Magnetometer.

The study area is about 250 meters long and 30 meters wide. We chose that region with the intention of testing the application's accuracy because its characteristics are well recognized. We surveyed the area where the sensors were applied completely on the ground, starting from west to east, where we had 26 profiles and 208 stations, and the distance was 4 meters station interval and 10 meters line spacing (Fig 3). The magnetic measurements and time were manually recorded in a notebook using the smartphone app and the magnetometer, and then put into an Excel sheet (Fig. 4).

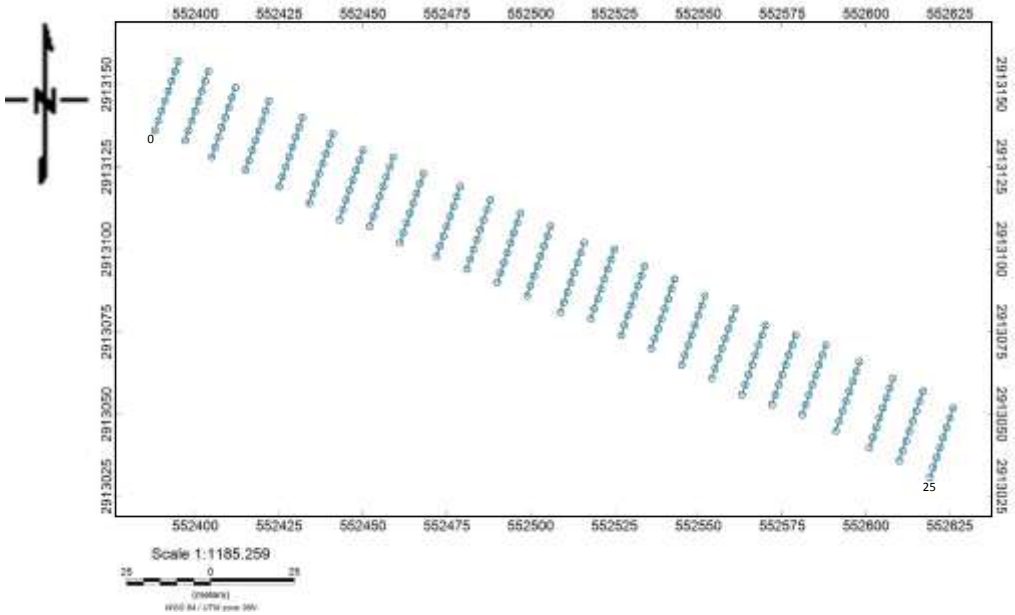

Figure 3: Layout of the magnetic survey using 10m line spacing and 4m station interval in Abu Marwat Concession.

Figure 4: Magnetic data acquisition using magnetometer and smartphone application.

We selected the Geosoft Oasis Montaj [7] (Version 8.4) software to evaluate and process the data. Since the data from the smartphone magnetic sensor is in micro tesla, we needed to convert them to nano tesla in order to calculate the statistical difference and compare it with magnetometer data in nano tesla because it is more accurate. The total magnetic intensity (TMI) map was created and the reduction to pole (RTP) map was used to rectify it. The radial average power spectrum (RAPS) and source power imaging (SPI) techniques were used to determine the depths of shallow and deep magnetic structures (e.g., faults). The statistical analysis was carried out by Microsoft Excel (version 365) where the data differences percentages, the median and the standard deviation have been calculated. On the following is a brief description of the applied filters and statistical analysis approach.

4.1 Reduction to the magnetic pole (RTP) technique

The idea behind this method is that the magnetization vector within the concealed causative body on the surface as well as the geomagnetic vector at observation points determine the amount and shape of created magnetic anomalies on the overall magnetic field. It is challenging to pinpoint the location of these bodies at low or moderate inclinations of the geomagnetic field because the peak of the maximum curvature generated by the body relocated away from over the center of the magnetized bodies. Therefore, it is advised to assess a hypothetical anomaly from the observed type on the total intensity map where the causal body can be directed as to be seen with respect to the magnetic north pole in order to ensure good accuracy of interpretation of the magnetic maps. Applying the reduction to magnetic pole procedures will result in the magnetization vector being roughly vertical [13].

4.2 Radial averaged power spectrum (RAPS)

Using Geosoft Oasis Montaj Version 8.4 [14], this approach was applied to gridded magnetic RTP data. In the RTP map's 2-D radially averaged power spectrum graphic, low wave values less than a certain cycle/km were employed to illustrate the deep-seated dispersion of sources. While the shallow source contribution keeps the wave number over a certain cycle/km threshold. A description of the 2-d power spectrum's interpretation. The lines (D), (S), and (N) depict the deeper anomaly sources, shallower sources, and noise signal, in that order. The following equation can be used to compute depth from the slope of the chart:

$$\text{depth} = -\text{slope}/4\pi$$

4.3 The source parameter imaging (SPI)

Source Parameter Imaging (SPI) is a method for automatically calculating source depths from gridded magnetic data [15]. The depth solutions calculated are recorded in a database. Because the depth measurements are independent of magnetic inclination and declination, a pole-reduced input grid is not required. This methodology is used to calculate the grid gradient amplitude in the X and Y axes to determine the depth to the basement. A 3x3 point convolution filter is used to compute the "x, y" derivatives. SPI uses a step-type source model and computes the "z" derivative using a one-step grid filtering operation to compute the first vertical derivative grid in the forward Fourier (frequency) domain transformation. An easy approach for determining the depth of magnetic sources with high accuracy (+/- 20%) and coherent solution points is Source Parameter Imaging (SPI). Similar to the Euler 3D deconvolution approach, this accuracy.

4.4 Statistical Analysis

A branch of mathematics, statistics which is a body of knowledge that deals with the gathering, examination, interpretation, and presentation of data. Instead of being a subfield of mathematics, some people view statistics as a separate mathematical discipline. Statistics is concerned with the use of data in the context of uncertainty and decision-making in the face of uncertainty, even though many scientific inquiries employ data [16].

In this study, we compared the results of the smartphone magnetic sensor and the magnetometer. We calculated the differences in TMI, RTP, RAPS and SPI values then the median and standard deviation of TMI, RTP, RAPS and SPI differences were evaluated, where the median is a type of average value, which describes the position of the center of the data, meanwhile, the standard deviation reflects the degree of dispersion of a set of values. A low standard deviation indicates that the values tend to be close to the mean of the set, while a high standard deviation indicates that the values are spread out over a wider range.

5- RESULTS and DISCUSSION

5.1 The total magnetic intensity (TMI)

The total magnetic field intensity maps produced from the magnetometer and smart phone magnetic sensor data are shown in figures 5a and b, respectively. The TMI map of magnetometer shows magnetic anomalies with magnitude values ranging from 42355.264 nT to 42435.785 nT (Fig. 5a). The TMI map of the smartphone magnetic sensor, on the other hand, displays magnetic abnormalities with magnitudes ranging from 38363.751 nT to 44456.455 nT (Fig. 5b). We can see that there are

disparities between the magnetic values from the magnetometer and the smartphone magnetic sensor. Both maps show that the northwest side of the anomalies' distribution is more contiguous than the southeast side. Moreover, the northwest sides of the study area display high magnetic values from 42417 nT to 42424 nT that may represent diorite lithology. Whereas the low magnetic values ranging from 42355 nT to 42371 nT may represent carbonate silica alteration.

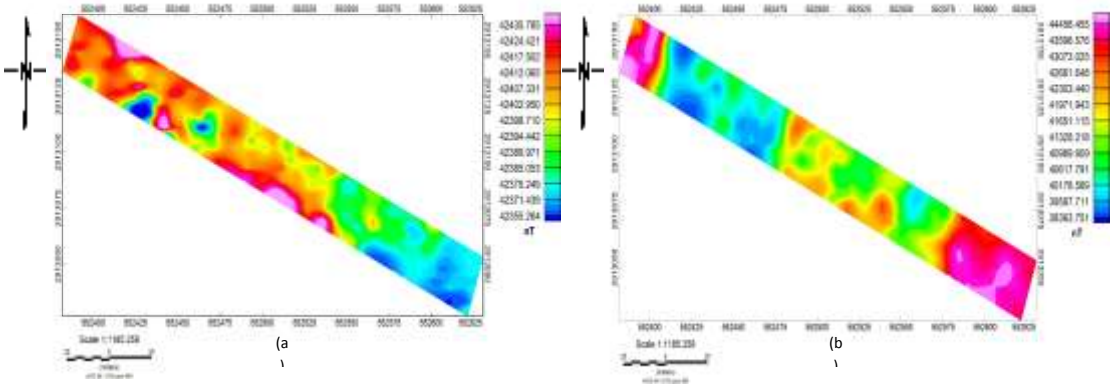

Figure 5: Total magnetic field intensity (TMI) map of the study area using (a) magnetometer and (b) smartphone magnetic sensor.

5.2 The reduction to magnetic pole (RTP)

The reduction to pole maps produced from the magnetometer and smart phone magnetic sensor data are shown in figures 6a and b, respectively. The RTP map that was produced from the magnetometer displays magnetic anomalies with magnitude values ranging from 42289.345 nT to 42497.739 nT (Fig. 6a). While Magnetic anomalies with magnitude values ranging from 34998.962 nT to 46584.472 nT are seen on the RTP map created by the smartphone magnetic sensor (Fig. 6b). The majority of the magnetometer's anomalies have been correctly positioned using the correct structure strike direction and the anomalies in the smartphone are also have been corrected slightly in the position with the right structure strike direction. As we notice that the trend structures strikes are southeast to northwest in both maps. The

high values that range from 42450 nT to 42498 nT in the magnetometer's map indicate a possible BIF structure beneath the highly sheared slates that we also can see the same anomaly in the smartphone sensor's map which the values range from 41860 nT to 43172 nT.

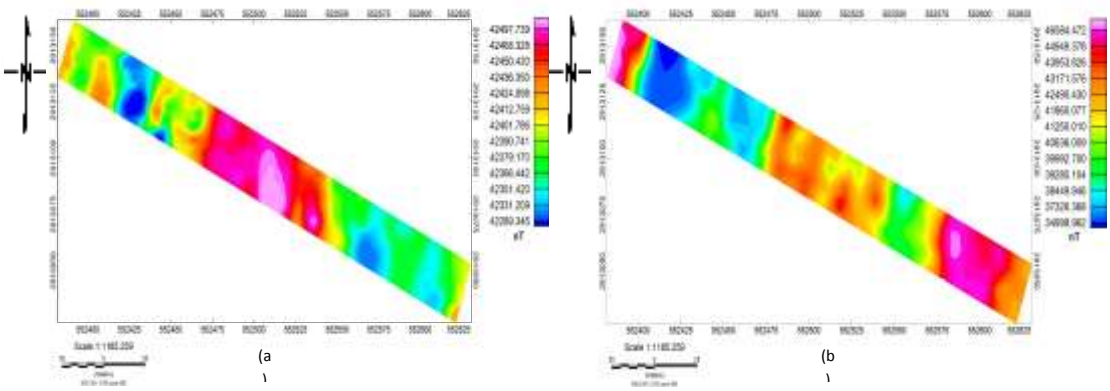

Figure 6: Reduction to pole (RTP) map of the study area using (a) magnetometer and (b) smartphone magnetic sensor.

5.3 The radially averaged power spectrum (RAPS)

The radially averaged power spectrum produced from the magnetometer and smart phone magnetic sensor data are shown in figures 7a and b, respectively. According to the RAPS that is produced from the magnetometer (Fig. 7a), It displays two major average levels at depths of -4 m and -9 m below the measurement level. While the RAPS obtained by the smart phone magnetic sensor displays two primary average levels at depths of -5 m and -13 m (Fig. 7b). We can conclude from the two RAPS results that there is proximity in shallow source average depths rather than those of the deep source. Though, the right selection of the slope for the various estimations is necessary for these results, for the relatively small variations of results in any direction.

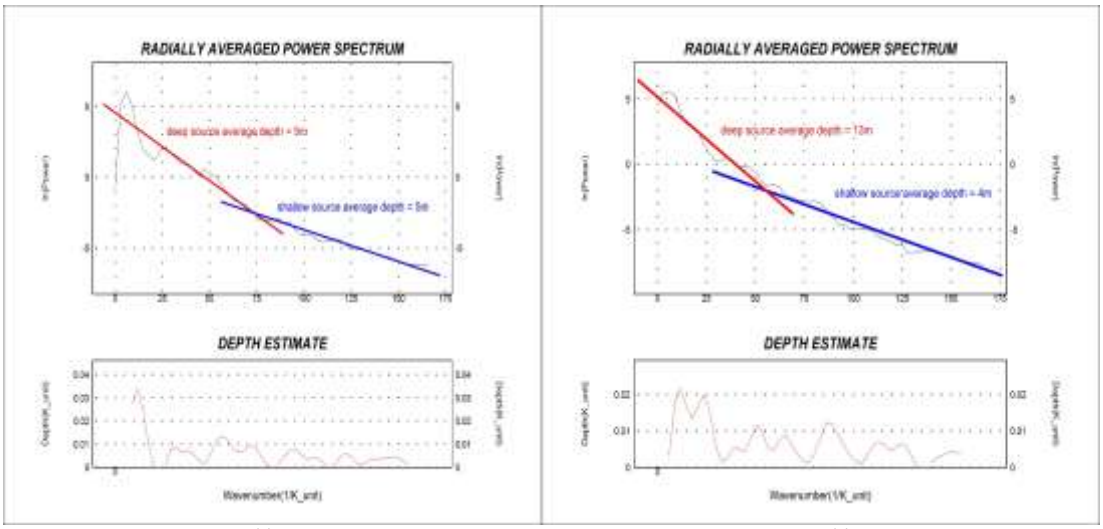

(a) (b)

Figure 7: Average depth estimation of magnetic anomalies at the study area using radial average power spectrum technique of (a) magnetometer and (b) smartphone sensor.

5.4 The Source parameter imaging (SPI)

The Source parameter imaging maps produced from the magnetometer and smart phone magnetic sensor data are shown in figures 8a and b, respectively. The SPI map of the research region obtained by the magnetometer shows that the depth of the linear anomalies ranges from -1.998 to -4.564 m (Fig. 8a), whereas the SPI map generated by the smartphone magnetic sensor shows that the depth of the linear anomalies ranges from 0.083 to -9.834 m (Fig. 8b), It also suggests, as demonstrated by RAPS, that shallow depths have greater propinquity than deeper depths.

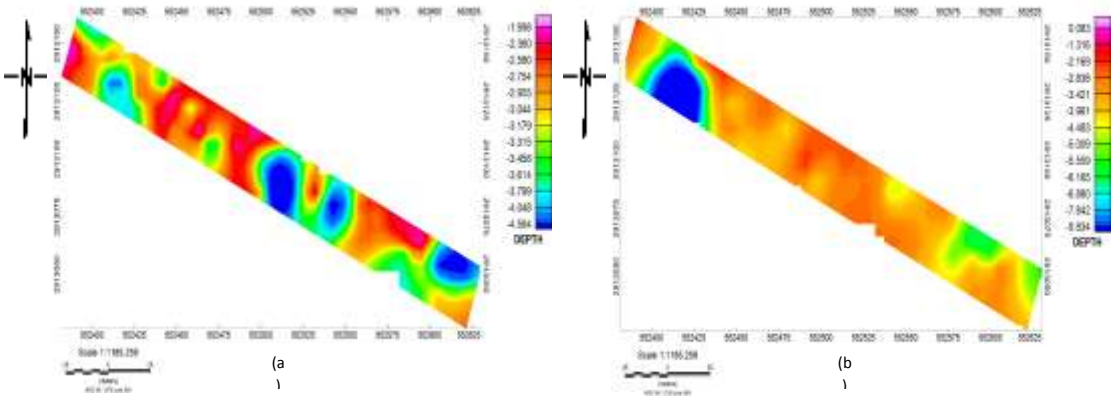

(a) (b)

Figure 8: Depth estimation using Source parameter imaging (SPI) technique of the study area of (a) magnetometer, (b) smartphone sensor.

5.5 Statistical Results

Most of the total magnetic intensity (TMI) differences percentages range from 91% to 100% with some differences scattering above the 100% up to 106% because we converted the micro tesla to nano tesla in smartphone sensor's readings that gives some unreal convergence (Fig. 9). But we found a high approximation in the median results 97.44% and the standard deviation was 3.97 which indicates that the values tend to be close to the mean.

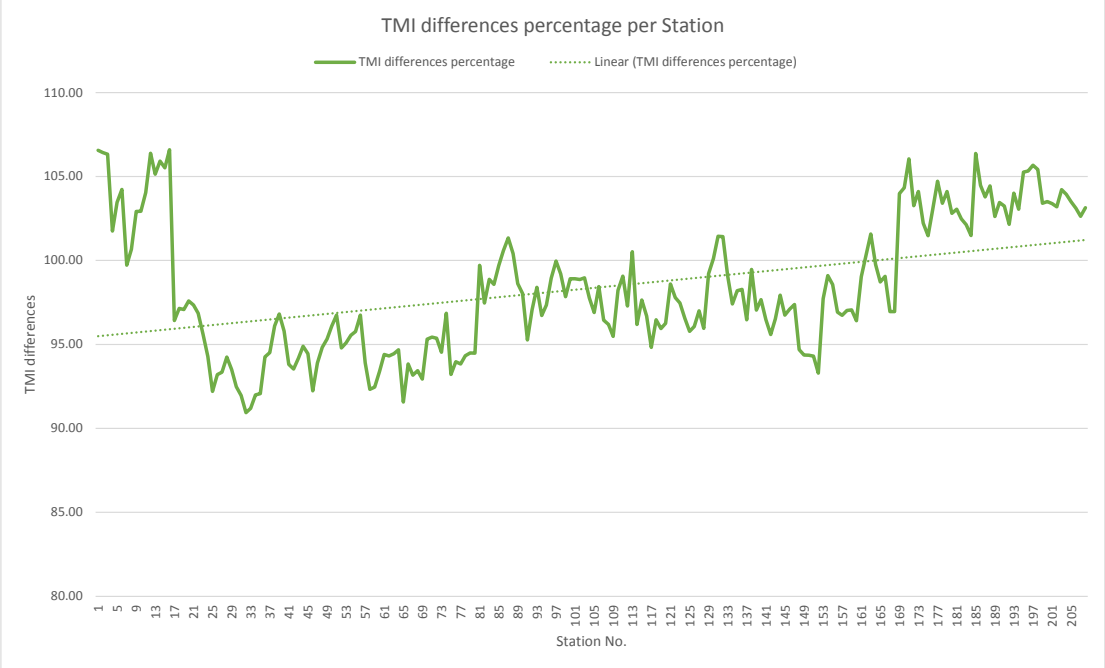

Figure 9: TMI differences percentage between smartphone and magnetometer.

The majority of reduction to pole (RTP) differences percentages range from 78% to 100% with some differences scattering above the 100% up to 117% because of the same reason as (TMI) (Fig. 10), that the RTP calculation took from it (Fig. 10). But we found a high approximation in the median results 98.44% and the standard deviation was 7.35 which indicates that the values tend to be close to the mean.

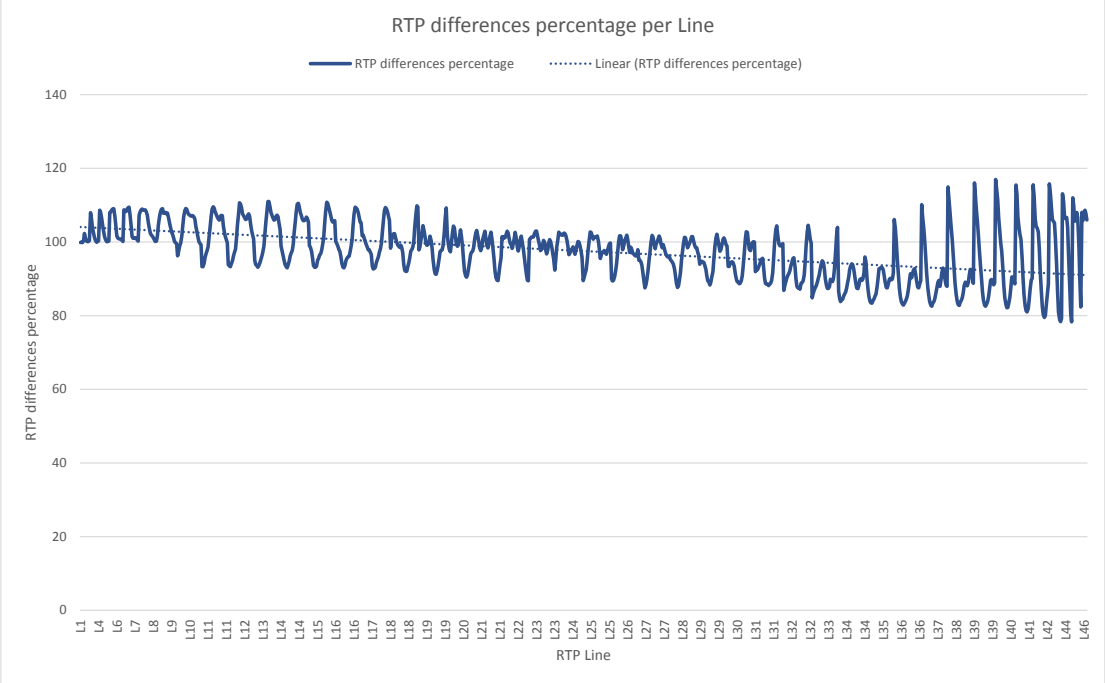

Figure 10: RTP differences percentage between smartphone and magnetometer.

The radially averaged power spectrum differences percentages are restricted between two values that controlled by shallow and deep depths, the shallow depths difference percentage is 80% where the depths are close to each other as we discussed in RAPS results before, but the deep depths difference percentage is 144.44% which is not real because there is a divergence in the depths. So due to the limitation of the values, the median is 112.22% and the standard deviation is 45.57 which is not reasonable and indicates that the values tend to be far from the mean.

The Source parameter imaging (SPI) differences percentages range from 10% to 100% with more differences scattering above the 100% up to 277.47% because the technique calculated the depths in the two maps in different locations not similar to each other which led to a high variation in the difference's percentages (Fig. 11). As we can see the median is 87.22% which gives us indication of a good approximation, but the standard deviation is 44.53 which indicates that the values tend to be far from the mean.

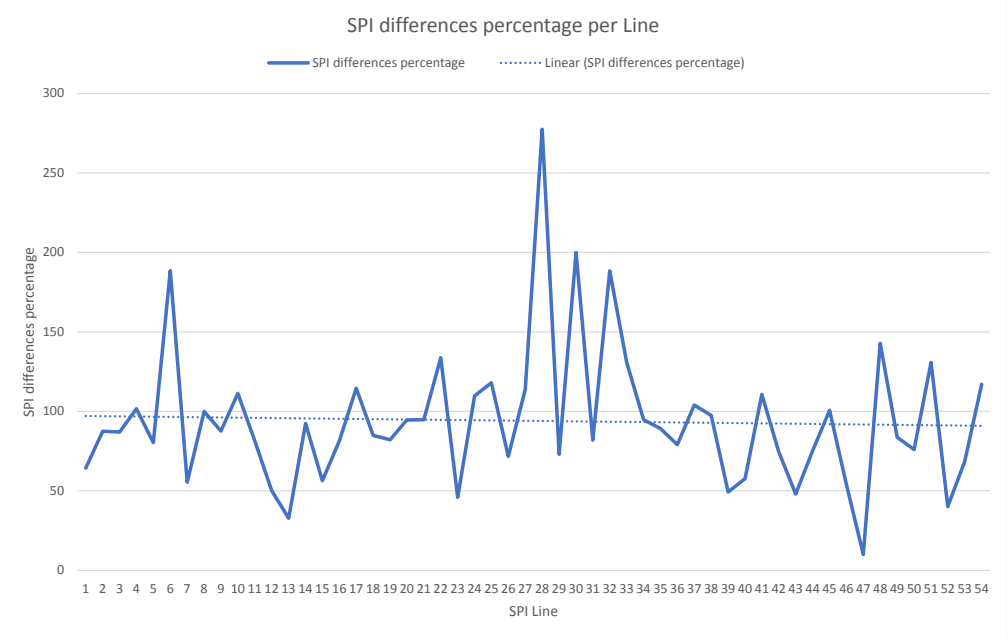

Figure 11: SPI differences percentage between smartphone and magnetometer.

6- Summary and Conclusion

The smartphone magnetic sensor (Physics toolbox magnetometer) was used to compare the capability and efficiency of the smart phone application to map the depths of shallow and deep subsurface magnetic features at Abu Marwat Concession in Egypt's Eastern Desert with the proton precession magnetometer (G-858). The resultant maps of TMI (magnetometer's magnitude values ranging from 42355.264 nT to 42435.785 nT and smartphone's magnitudes ranging from 38363.751 nT to 44456.455 nT), RTP (magnetometer's magnitude values ranging from 42289.345 nT to 42497.739 nT and smartphone's magnitudes ranging from 34998.962 nT to 46584.472 nT), RAPS (magnetometer's average levels at depths of -4 m and -9 m and smartphone's average levels at depths of -5 m and -13m) and SPI (magnetometer's depth of the linear anomalies ranges from -1.998 to -4.564 m and smartphone's depth of the linear anomalies ranges from 0.083 to -9.834 m) showed that the sensitivity of the magnetometer is higher than the smartphone magnetic sensor in detecting the depths of the deeper features e.g., faults. Meanwhile regarding shallow depths, the

smartphone magnetic sensor's ability to detect the geological features was on the same scale as that of the magnetometer. Therefore, using a smartphone magnetic sensor is highly recommended for estimating shallow depths due to its affordability, simplicity, and portability. In the future, it will be worthwhile to create a revolutionary mobile application capable of processing acquired geophysical data, mapping the magnetic anomaly, and finally providing the depth and shape of the magnetic body.

REFERENCES

[1]. A. Khalil, T. H. Abdel Hafeez, H. S. Saleh, and W. H. Mohamed, Inferring the subsurface basement depth and the structural trends as deduced from aeromagnetic data at West Beni Suef area, Western Desert, Egypt. NRIAG Journal of Astronomy and Geophysics, 5, (2016) 380–392.

[2]. H. S. Mohamed., M. M. Senosy, and M. Abdel Zaher, Interactive interpretation of airborne gravity, magnetic, and drill-hole data within the crustal framework of the northern Western Desert, Egypt, Journal of Applied Geophysics 134 (2016) 291–302.

[3]. A. S. Abu El-Ata, A. A. EI-Khafeef, S. E. Ghoneimi, S. H. Abd Alnabi, and M. A. Al-Badani, Applications of aeromagnetic data to detect the Basement Tectonics of Eastern Yemen region, Egyptian Journal of Petroleum, 22, (2013) 277-292.

[4]. J. Reynolds, An introduction to applied and environmental geophysics, John Wiley and sons, Chester, 2nd edition, (1997) 710 p.

[5]. W. D Jones, Compass in Every Smartphone, IEEE Spectrum, Vol. 47, No. 2, (2010) pp. 12-13.

[6]. H. Ketabdar, A. Jahanbekam, K. A. Yuksel, T. Hirsch, and A. A Haji, Magi Music: Using Embedded Compass (Magnetic) Sensor for Touch-Less Gesture Based Interaction with Digital Music Instruments in Mobile Devices," Proceedings of the 5th International Conference on Tangible, Embedded, and Embodied Interaction, Funchal, 22-26 January 2011, (2011) pp. 241-244.

[7]. M. Eraky, G. Abdelaal, and A. El-Haddad, Detection of Depth and Location of Subsurface Utilities Using Smart Phone Magnetic Application: A Case Study at Assiut University, Egypt", Assiut University J. of Geology, 1(1), (2022) pp175-190.

[8] M. Ndiaye, and A. Diagne, Geomagnetic Investigation Method Using iPhone® Integrated Magnetic Sensor. International Journal of Geosciences, (2014) 5, 1-4.

[9] N. Campbell, E. Atekwana, A. J. Mathews, and A. Ismail; Geophysical applications of magnetic sensors in smartphones. The Leading Edge (2020); 39 (5): 312–317.

[10] C. Vo, S. Staples, D. Cowell, B. Varcoe, S. Freear, and C. Cookson, Determining the Depth and Location of Buried Pipeline by Magnetometer Survey. Journal of Pipeline Systems Engineering and Practice, (2020) 11 (2).

[11] E. O. Joshua, G. O. Layade, V. Akinboboye, and S. A. Adeyemi. Magnetic mineral exploration using ground magnetic survey data of Tajimi Area, Lokoja." Global Journal of Pure and Applied Sciences 23 (2017): 301-310.

[12]. T. Neall, Notes on the Geology of the Rodruin deposit and its immediate area (2023) (unpublished internal report Aton Resources Inc.)

[13] V. Baranov, A New Method for Interpretation of Aeromagnetic Maps, Pseudo-Gravimetric Anomalies. Geophysics, (1957) 22, 359-363.

[14]. J.B. Thurston and R.S. Smith, Automatic Conversion of Magnetic Data to Depth, Dip, and Susceptibility Contrast Using the SPITM Method. Geophysics, 62, (1997) 807-813.

[15]. G. Z. Abdelaal, A. E. El-Haddad, M. S. Badri and M. A. Mohamed, Inferring Depth to Basement Using Airborne Magnetic Data at Wadi El Nakhil Area, Eastern Desert, Egypt, Assiut University J. of Geology, 48(1), (2019) pp1-11.

[16]. L. E. Moses, Think and Explain with Statistics, Addison-Wesley, (1986) pp. 1–3